PHYSICAL REVIEW VOLUME 121, NUMBER 5 MARCH 1, 1961

Magnetic Interaction of Cerium and Cobalt Ions in Double Nitrate Crystals[*]

J. W. CULVAHOUSE, W. UNRUH,[†] AND R. C. SAPP
Department of Physics and Astronomy, University of Kansas, Lawrence, Kansas

(Received August 22, 1960)

The space group of the double nitrate crystals $M_2'M_3''(NO_3)_{12}\cdot 24H_2O$, where M' is a trivalent cation and M'' is a divalent cation, has been determined from x-ray data to be $R\bar{3}m$. The rhombohedral unit cell has sides of 13.1 A, interaxial angles of 49° and contains one molecule. The cerium ions have the locations $\pm(\frac{1}{4},\frac{1}{4},\frac{1}{4})$. The line shapes of the derivative with respect to magnetic field of the paramagnetic resonance absorption of small concentrations of cobaltous ions substituted in $Ce_2Zn_3(NO_3)_{12}\cdot 24H_2O$ are described and used to determine the spatial relations of the cerium ions and cobalt ions, as well as to justify the assumption of a dipolar interaction between them described by the spin Hamiltonian parameters of the cerium and cobalt ions. It is concluded that the more isotropic of the two paramagnetic spectra of cobalt ions observed in this salt is due to ions in either the special sites $\pm(0.399,0.399,0.399)$ or, rather less likely, in the special sites $\pm(0.101,0.101,0.101)$ and that the highly anisotropic spectrum of cobalt ions is due to ions in the body-centered site.

I. INTRODUCTION

The double nitrate crystal $Ce_2Mg_3(NO_3)_{12}\cdot 24H_2O$ (Ce−Mg) has been a very useful paramagnetic cooling agent[1] and is particularly suitable for orientation of the nuclei of divalent ions of the Fe group.[2] The interpretation of many of the nuclear orientation experiments has been hampered by a lack of knowledge of the nature of the spin-spin interactions between the divalent ions and the cerium ions[3,4] which function as the paramagnetic cooling agent. Recent work has shown that this effect is very important for the orientation of small concentrations of cobalt nuclei in Ce−Zn.[5]

The lattice of the cerium ions was established at the time of the earliest work on the paramagnetic resonance[6]: Nuclear magnetic resonance measurements of the proton spectra due to the water molecules[7] and paramagnetic resonance studies of radiation damage effects[8] have been advanced as evidence for the position of the water molecules and nitrate ions relative to the cerium or more generally the trivalent positions. To our knowledge, the only speculation also concerned with the divalent positions is that of Hellwege and Hellwege[9] who were concerned with the explanation of optical absorption in the isomorphous crystal Pr−Zn.

The primary purpose of this paper is to establish the nature of the spin-spin interaction between cerium ions and cobalt ions placed in the trivalent and divalent sites of this salt. One may view this problem as having two distinct aspects: the spatial relations of the cerium and cobalt ions and the Hamiltonian which describes the interactions. It is assumed from the outset that this Hamiltonian is just the interaction energy between two magnetic dipoles which are related to the effective spin of the ions by the spin Hamiltonian parameters deduced from the Zeeman energy levels. This assumption is plausible for dissimilar ions but, to our knowledge, has not been demonstrated quantitatively.

The problem has been approached as follows: x-ray powder diffraction data were analyzed to obtain the size of the unit cell and the space group of the double nitrate crystals. These data limit the possible divalent positions in the unit cell to a very few choices. With these limitations in view, the divalent sites could be identified by the shape of the paramagnetic absorption spectra in Ce−Zn crystals containing about 1% of cobalt substituted for zinc. This identification is dependent upon the assumption of dipole-dipole interaction discussed above but the detailed agreement of experiment and theory strongly supports this assumption.

In Sec. II, the paramagnetic spectrometer is described and the general features of the paramagnetic resonance spectra of cobalt ions in (La+Ce)−Zn are discussed for various ratios of lanthanum and cerium. Finally the curves obtained for the derivative with respect to magnetic field of the paramagnetic absorption —in the future these will be referred to as line shapes— are discussed and interpreted in terms of the cerium environment. Section III contains a quantitative comparison of the observed line shapes with those expected for the possible divalent sites. A unique solution is found and a more detailed comparison is presented to strengthen the assumption of dipolar interaction.

II. ELECTRON PARAMAGNETIC RESONANCE MEASUREMENTS

Paramagnetic Spectrometer

The spectrometer used for these measurements operates in the 12.4 to 18.0 kMc/sec frequency band.

---

[*] This work was supported in part by the National Science Foundation and the Office of Naval Research.

[†] Socony-Mobil Fellow for 1959-60.

[1] J. M. Daniels and F. N. H. Robinson, Phil. Mag. **44**, 630 (1953).

[2] C. S. Wu *et al.*, Phys. Rev. **105**, 1413 (1957).

[3] J. C. Wheatley *et al.*, Physica **21**, 841 (1955).

[4] P. S. Jastram, R. C. Sapp, and J. G. Daunt, Phys. Rev. **101**, 1381 (1956).

[5] M. W. Levi, R. C. Sapp, and J. W. Culvahouse, Phys. Rev. **121**, 538 (1961).

[6] A. H. Cooke, H. J. Duffus, and W. P. Wolf, Phil. Mag. **44**, 623 (1953).

[7] T. L. Estle, H. R. Hart, and J. C. Wheatley, Phys. Rev. **112**, 1576 (1958).

[8] B. Bleaney, W. Hayes, and P. M. Llewellyn, Nature **179**, 140 (1957).

[9] A. M. Hellwege and K. H. Hellwege, Z. Physik **135**, 92 (1953).

It utilizes a reflection-type sample cavity which can be immersed in a liquid helium bath. The helium bath can be pumped to produce temperatures between 4.2° and 1.1°K. A balanced mixer is used for superheterodyne detection with a 30-Mc/sec i.f. In one mode of operation, the transmitter klystron is locked to an auxiliary cavity and the local oscillator frequency is locked 30 Mc/sec away from the transmitter frequency. The sample cavity is placed in one arm of a magic tee bridge which can be adjusted to measure either paramagnetic dispersion or absorption. In another mode of operation, the transmitter klystron is locked to the center of the sample cavity mode and only paramagnetic absorption is measured.

The static magnetic field H_0 is supplied by a 12-in. Varian electromagnet with a rotating yoke. The field is modulated at a frequency of 31 cps by auxiliary coils wound on the pole tips. The modulated signal from the i.f. strip is fed to a conventional lock-in-mixer and the dc output is recorded on a Varian strip-chart recorder. Field sweeps are generated by applying the output of a motor-driven Helipot voltage divider to the sweep input of the Varian magnet power supply. Field markers are inserted manually by observing an oscilloscope display of the proton magnetic resonance.

General Features of the Spectra of Cobalt Ions in the Double Nitrates

The paramagnetic resonance spectra of cobalt ions substituted for approximately 1% of the zinc ions in La−Zn are very similar to those which have been obtained in La−Mg and Bi−Mg.[10] Spectra due to two types of cobalt sites are observed which have been designated the *X* and *Y* ions.[11] Both ions have effective spin ½ and axial symmetry about the trigonal axis of the crystal and are described by the spin Hamiltonian

$$\mathcal{H}=g_{\parallel}\beta S_zH_z+g_{\perp}\beta(H_xS_x+H_yS_y)+AI_zS_z+B(I_xS_x+I_yS_y).$$

The spin Hamiltonian parameters obtained for this compound at a temperature of 4.2°K are listed in Table I. These results show that the *X* ion is more nearly isotropic than has been found in other salts of this series. The *X*-ion spectrum consists of eight hyperfine lines that are very nearly equally spaced with a separation of about 48 gauss. The *Y*-ion spectrum is highly anisotropic, and the hyperfine structure ranges from eight lines spaced at 85-gauss intervals when the field is applied along the symmetry axis to four unequally spaced lines when the field is perpendicular to this axis. This behavior of the *Y*-ion spectra complicates the analysis of line shapes for crystals containing cerium. The individual hyperfine components of both the *X* and *Y* ion have full widths at half maximum of about 15 gauss.

TABLE I. Spin Hamiltonian parameters for cobalt ions in $(La+Ce)_2Zn_3(NO_3)_{12}\cdot 24H_2O$.

% Ce	$g_{\parallel}$	$g_{\perp}$	$A\times10^4$ cm^{-1}	$B\times10^4$ cm^{-1}
		(a) Cobalt ions in the *X*-ion site		
0	4.37±0.01	4.31 ±0.01	98.9±0.5	94.5±0.5
10	4.36±0.01	4.30 ±0.01	98.6±0.5	94.8±0.5
50	4.35±0.02	4.30 ±0.02	95.0±2.0	95.0±2.0
100	4.34±0.04	4.28 ±0.04	95.0±2.0	95.0±2.0
		(b) Cobalt ions in the *Y*-ion site		
0	7.36±0.01	2.337±0.005	292± 1	≤ 3
10	7.35±0.01	2.34 ±0.01	291± 1	≤ 3
50	7.21±0.06	2.37 ±0.03	280± 9	≤10
100	7.18±0.10	2.38 ±0.08	291±15	≤30

Bowers and Owen[12] report that the ratio of the number of *X* ions to the number of *Y* ions is 1.6:1. We have obtained (1.8±0.2):1 for this ratio in the one sample for which careful intensity measurements were made.

The spin Hamiltonian parameters are listed in Table I for double nitrate salts in which an increasing fraction of the lanthanum was replaced by cerium. A small but systematic change with cerium concentration appears to be present, although the error increases considerably at the high cerium concentrations due to the complicated line shapes.

The resonance spectrum of the cerium ion in these compounds is described by an effective spin ½ and, like the cobalt ions, has axial symmetry about the trigonal axis of the crystal. Our measurements of the cerium resonance in Ce−Zn have yielded the spin Hamiltonian parameters $g_{\perp}=1.82\pm0.01$ and $g_{\parallel}\leq0.25$ which is in agreement with paramagnetic resonance measurements on Ce−Mg.[6] There is no hyperfine structure because the cerium nucleus has zero spin. We have not attempted to understand the linewidth of the cerium resonance in Ce−Zn which is wider than that previously reported for Ce−Mg.[6] When the field is applied perpendicular to the symmetry axis, the separation of the points of maximum slope is 125 gauss. If, as appears, the line shape is Gaussian, this would correspond to an rms width of 62.5 gauss. For field directions away from the symmetry axis, the line broadens in a magnetic field display almost inversely with the effective *g* value. One may infer that the spin-spin relaxation time is no shorter than 1.5×10^{-9} sec for any field direction more than 30° away from the symmetry axis. This will be a lower limit for the correlation time of the magnetic fields produced by the component of the cerium spin along the precession axis of the cerium. These fields will be essentially static for the cobalt ions.

Observed Line Shapes for the *X* Ion

The derivative with respect to magnetic field of the paramagnetic resonance absorption of cobalt ions of

---

[10] W. B. Gager, P. S. Jastram, and J. G. Daunt, Phys. Rev. **111**, 803 (1958).

[11] R. S. Trenam, Proc. Phys. Soc. (London) **A66**, 118 (1953).

[12] K. D. Bowers and J. D. Owen, *Reports on Progress in Physics* (The Physical Society, London, 1955), Vol. 18, p. 304.

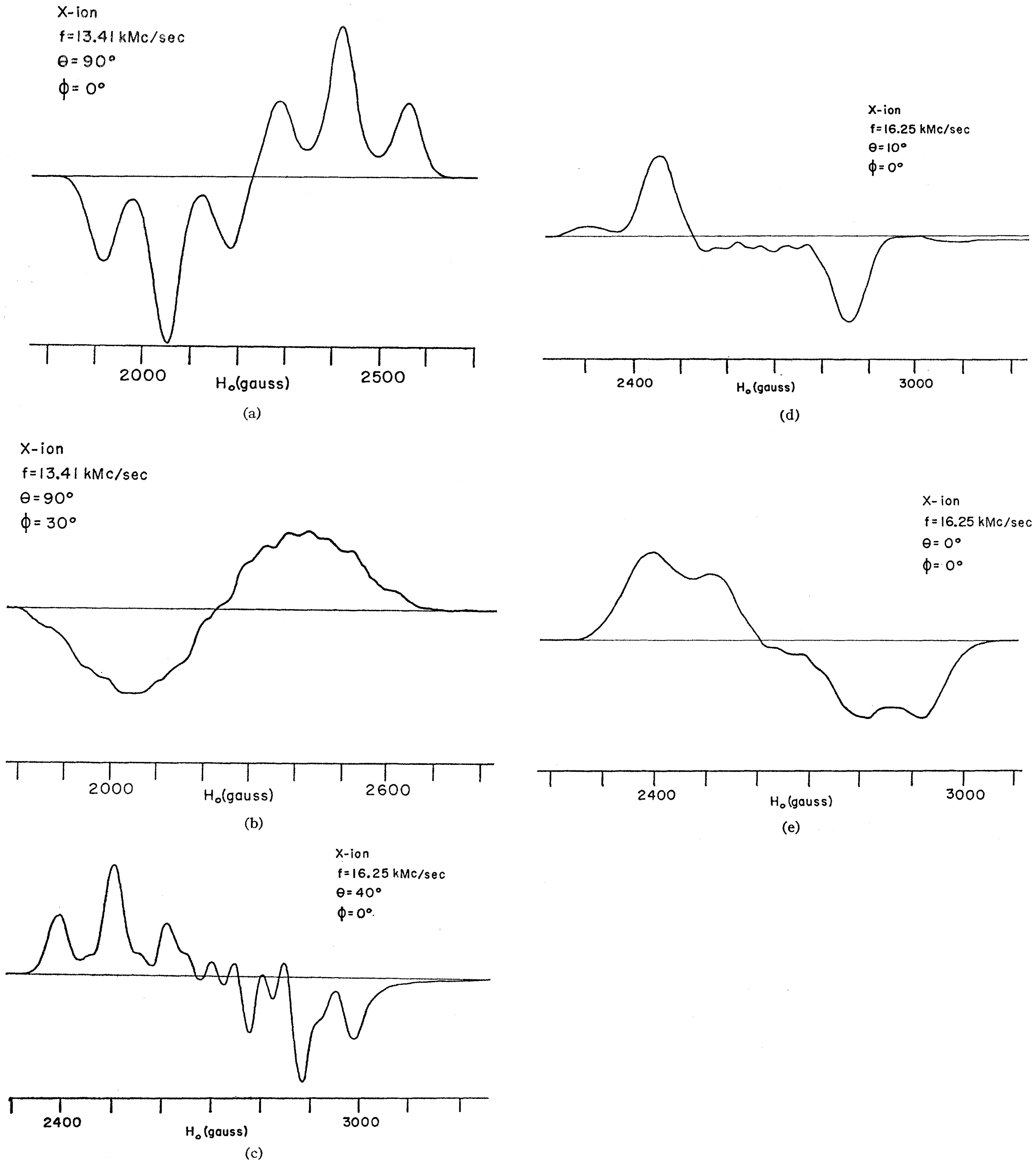

FIG. 1. The derivative with respect to magnetic field of the paramagnetic absorption for the X ion for five different directions of the applied field. θ and ϕ are the polar and azimuthal angles for the field direction which are defined at the beginning of Sec. II, f is the klystron frequency, and H_0 is the applied field.

low concentration in Ce—Zn has been recorded for a large number of directions of the applied magnetic field. The magnetic field direction is specified by the polar angle θ measured away from the trigonal axis of the crystals, which is perpendicular to the plane of the flat hexagonal plates in which these crystals grow, and an azimuthal angle ϕ measured away from an axis perpendicular to one of the six sides of the hexagonal plates. The error in these angles due to misorientation of the crystal is less than ±2.5°.

A few of the observed line shapes are presented in Figs. 1 and 2. These curves are tracings of recorder charts. Although the time constant used for these measurements was less than 1 sec, almost no noise was

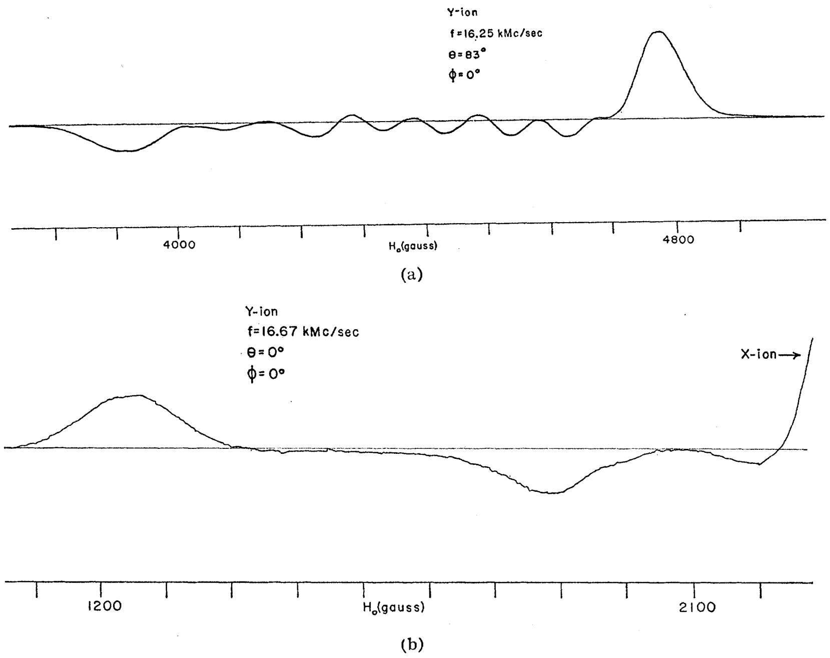

FIG. 2. The derivative with respect to magnetic field of the paramagnetic absorption for the Y ion for two different directions of the applied field. The symbols are the same as those in Fig. 1.

present. The major error in these curves arises from recorder deadband which sometimes was 1% of the total extent of the curves. Some of the shapes may be distorted slightly by the presence of paramagnetic dispersion. Care was taken to eliminate distortion due to excessive modulation amplitude and saturation effects. The magnetic field sweep was slightly nonlinear but this has not been taken into account in the abscissa scale of the figures, as it seldom amounts to more than a 5% change in the sweep rate over a 500-gauss range and is usually less. In the analysis of the data, corrections were made for sweep nonlinearity.

Figure 1(a) is the line shape obtained for the X ion for $\theta=90°$, $\phi=0°$. To analyze the implications of this shape one must refer to the curves presented in Fig. 3. The curves presented there are obtained by adding together the derivatives of eight equally spaced Gaussian curves, for several values of the rms width of the Gaussian components relative to the spacing. The use of these curves in deducing hyperfine spacings and rms widths of the components is discussed in Appendix I. Comparison of the curves in Fig. 3 and Fig. 1(a) suggests that the latter is a superposition of three of the calculated curves, a central one and two others, one-half as intense, which are shifted up and down in field by 135±3 gauss. This situation will arise if two of the cerium neighbors are exceptionally effective in producing a component of field in the direction of the applied field at the position of the X ion. Two such cerium neighbors will have a total of four spin states. From the relative intensities it appears that two of these states correspond to a very small field at the X-ion site and the other two states correspond to fields of ±135 gauss. As a further check on this interpretation, the derivative of absorption was obtained for the X ion in a crystal containing 50% Ce and 50% La. In this case one observes a large central component, somewhat weaker components at ±68 gauss and very weak components at ±135 gauss. The lines at ±68 gauss arise from sites where one of the important trivalent positions is occupied by a cerium ion and the other by a lanthanum ion. The relative intensities of the components were very nearly 1:4:6:4:1, as would be expected on the basis of the multiplicity of spin states and an occupation probability of $\frac{1}{2}$ for cerium ions in a trivalent site. The two nearest neighbors do not need to be equivalent but the fields which they produce at the X-ion site in the direction of the applied field must be the same within about 20%; otherwise, more structure would be observed.

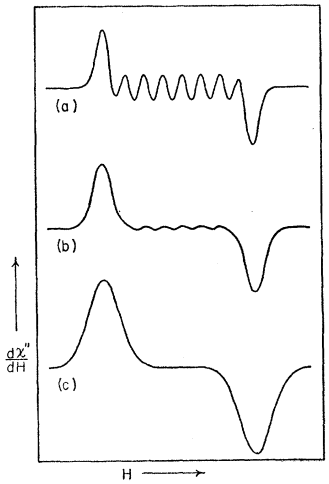

FIG. 3. Curves for the derivative of eight equally spaced Gaussian lines. The ratio of the rms width of the Gaussian components to the spacing is 0.438 for (a), 0.585 for (b), and 0.875 for (c). The paramagnetic absorption is proportional to the imaginary part of the susceptibility χ'', the derivative of which is used as the ordinate in this figure.

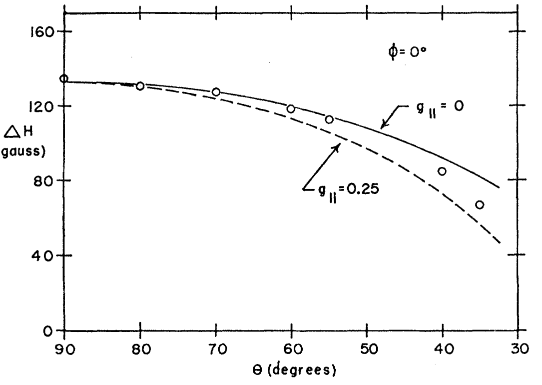

FIG. 4. The splitting of the components of the X-ion resonance as a function of θ for $\phi=0$. See the beginning of Sec. II for a definition of θ and ϕ. The curves are the theoretical results assuming that the cobalt ion is in the special site shown in Fig. 7(c), and assuming the two values indicated for $g_{\|}$ of the cerium ion. The errors in ΔH are less significant than a possible error of ±2.5° in the angles.

The line shape has been investigated by varying ϕ through 90° in steps of 5° while θ was held at 90°. The well defined components observed at $\phi=0°$ rapidly become obscured until, at $\phi=30°$, one observes the curve reproduced in Fig. 1(b). There is structure in this curve, although it is due to a larger number of neighbors which produce comparable fields at the X ion. The line shape has a 60° periodicity in the angle ϕ, and Fig. 1(a) is reproduced for $\phi=60°$. This is the minimum periodicity expected because of the threefold symmetry of the crystal.

With ϕ held at zero, θ has been varied by 120° in 5^0 steps. The results at 40°, 10° and 0° are reproduced in Fig. 1(c), (d), and (e). The most striking feature is the decrease of the distance from the central peak to the side peaks as well as a general narrowing of the structure. The splitting ΔH measured from the central peaks to the side peaks has been plotted in Fig. 4 over the range of angles for which it could be accurately measured. The curves drawn in Fig. 4 are according to the theory presented in Sec. III.

We have also calculated σ_d^2, the mean square magnetic field width due to interactions for these curves, by calculating the second moment of the observed line relative to the average value of the magnetic field and subtracting the second moment about the average field due to the hyperfine structure. The correctness of this procedure can be demonstrated if the interactions produce a symmetrical broadening, which is expected if the cerium ions are not significantly polarized. Under the conditions of this measurement, the polarization of the cerium ions was about 5%. Values of the σ_d, the rms magnetic field width, thus obtained are plotted in Fig. 5 as a function of ϕ when $\theta=90°$, and in Fig. 6 as a function of $\sin\theta$ when $\phi=0$. The curves in these figures are the theoretical results discussed in Sec. III. It is interesting to note that the rms width changes very little with ϕ despite the drastic change in the line shape. The errors in σ_d are difficult to estimate. From the scatter of the experimental points in Fig. 5, one may estimate the probable error in σ_d to be six gauss for $\theta=0°$. The magnitude of the error should remain nearly constant at all values of θ. The error bars in Fig. 6 are based on this assumption.

One might expect σ_d to decrease with decreasing θ in the way that it does because the g factor which gives the Zeeman splitting is practically proportional to $\sin\theta$. When σ_d is calculated by either the method of Pryce[13] or the method described in Sec. III, it is found to be almost exactly proportional to the above g factor. This result is not general as it depends upon the distribution of neighbors.

The second moments of the X-ion resonance have not been calculated for θ less than 30° because of the great complications of the line shapes at smaller angles. This complication arises because the g factor for the cerium ions becomes so small that the satellite lines due to simultaneous transitions of the cerium and cobalt spins are not clearly separated from the main resonance. These satellite lines are apparent in Fig. 1(d) where a bump is observed on the low and high sides of the main structure. Each of these bumps may be interpreted as the outer peak of a set of overlapping hyperfine lines similar to the main set of lines. The second peak of each set is obscured by the main line.

For ordinary dipolar interactions, without the complication of anisotropic g factors, one expects satellite lines corresponding to the g factors $g'\pm g''$ and $g'\pm 2g''$, where g' is the cobalt g factor and g'' is that for the cerium ion.[14] In this case, the satellite will have the same hyperfine structure—measured in units of frequency—as the main line and will have the cerium linewidth folded in. The intensity of the satellites is inversely proportional to the square of the distance that they are away from the main line (again measured in frequency units). From perturbation calculations,

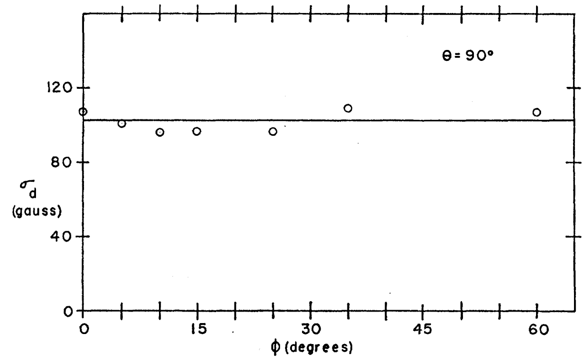

FIG. 5. The rms magnetic field width due to interactions of the X ion as a function of the azimuthal angle ϕ. The line is the theoretical result obtained in Sec. III. It is believed that this curve defines the precision of the second moment calculations.

---

[13] M. H. L. Pryce and K. W. H. Stevens, Proc. Phys. Soc. (London) **A63**, 36 (1950).

[14] R. Kubo and K. Tomita, J. Phys. Soc. Japan **9**, 888 (1954).

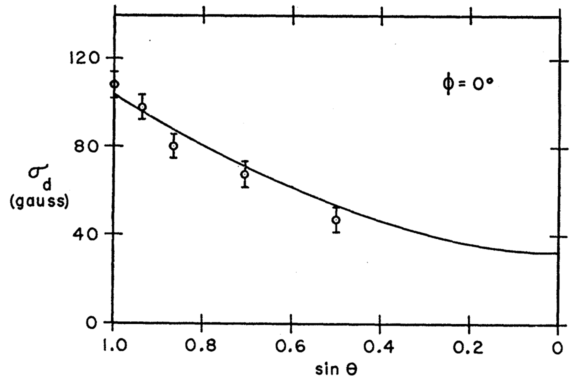

FIG. 6. The rms magnetic field width due to interactions for the X ion as a function of sinθ. The curve is the theoretical result obtained in Sec. III by assuming $g_{\parallel}=0$.

valid when $g''\beta H_0$ is large compared with the strength of the interactions, it is apparent that the same effects occur for anisotropic g factors but the detailed evaluation of the relative amplitude of the satellites is more involved.

The satellite lines in Fig. 1(d) were first observed at $\theta = 20°$ and were observed to move in closer to the main line and grow stronger. The low-field satellite is closer in field than the high-field line as is in accord with the above discussion. Also the closer one of the satellites is stronger. If a frequency sweep rather than a magnetic field sweep could be made, the satellites would be symmetrically located and equally strong. The g factors obtained for the satellites and main component in Fig. 1(d) are 4.03, 4.33, 4.66. This corresponds to a g factor of 0.32 ± 0.06 for the cerium ion at $\theta = 10°$ which is in accord with the limit $g_{\parallel} \leq 0.25$ deduced from direct measurement of the cerium resonance.

We were not able to resolve the more distant satellite, which in an isotropic powder would be about one-fourth as strong as the closer one. It is no doubt included in Fig. 1(e).

The presence of satellites at $\theta = 0$ complicates any attempt to determine the relative number of X and Y ions in a crystal containing cerium, a measurement that would be of some help in the interpretation of nuclear orientation experiments. If one attempts to determine the X to Y ratio at large values of θ, the highly anisotropic g value of the Y ion requires that one know very accurately the direction of the rf magnetic field in the crystal in order to evaluate the transition matrix elements.

Observed Line Shapes for the *Y* Ion

Investigation of the Y ion is more difficult than for the X ion for the following reasons: For θ between 90° and 75°, the Y-ion spectrum is well separated from that of the X ion but there is a very prominent second-order effect so that the lines are not equally spaced. Between 75° and 50°, the much weaker Y-ion resonance overlaps that of the X ion and, while it is not difficult to correct the X-ion data for this effect, very little can be learned from the Y-ion spectra in this range of angles. For angles smaller than 45°, the lines shapes are already complicated by the overlap with satellite lines because of the large g value and hyperfine splitting.

In Fig. 2(a) the nature of the hyperfine structure is apparent. The large second order effect leads to a rapidly increasing spacing at the low-field end. It is apparent from this curve that there are no prominent nearest neighbor effects. At $\theta = 0°$, the satellites are less resolved than for the X ion, as is expected. The extra width of the high-field peak in Fig. 2(b) is probably due to the larger separation of the satellites at higher fields.

The extraction of the mean square magnetic field width due to interactions for these curves is complicated by the fact that the hyperfine contribution varies rapidly with angle and is usually large. At $\theta = 90°$, the hyperfine contribution is fairly small and the uncertainty in the exact position of the trigonal axis is not so important. The value of σ_d in gauss for $\theta = 90°$ is found to be 85 with an upper limit of 98 and a lower limit of 64.

III. DETERMINATION OF THE DIVALENT SITES

From the x-ray data discussed in Appendix II, the unit cell for the double nitrates is found to be a rhombohedron with sides of 13.1 A and interaxial angle of 49°. The long diagonal of the rhombohedron is along the trigonal axis of the crystal and is 34.18 A long. There are two trivalent ions along this diagonal and 8.54 A to either side of the center of the cell. Only two arrangements of the three divalent ions are consistent with the space group $(R\bar{3}m)$[15]: (a) three divalent ions on the face centers of the rhombohedron, and (b) one divalent ion at the body center and two at special positions $\pm(x,x,x)$ which are along the long diagonal of the rhombohedron and $34.18x$ A to either side of the center of the cell.

The nearest cerium neighbors of the three possible cobalt sites are shown in Fig. 7(a), (b), and (c). The field produced by these neighbors in the direction of an applied field may be calculated assuming that the component of the cerium spin along its precession axis is essentially static for the production of fields seen by cobalt ions. The precession axis for the cerium ions is the same as the applied field direction only for $\theta = 0°$ and $\theta = 90°$. The observed splittings ΔH for the X ion are assumed to represent the component of this field that is in the direction of the applied field. It will also be assumed that the two cerium spin states are equally occupied, which, as pointed out previously, is a good approximation at 4.2°K. Some data taken at 1.1°K will be discussed later where this assumption is modified.

---

[15] *International Tables for X-Ray Crystallography* (Kynoch Press, Birmingham, 1952), p. 273.

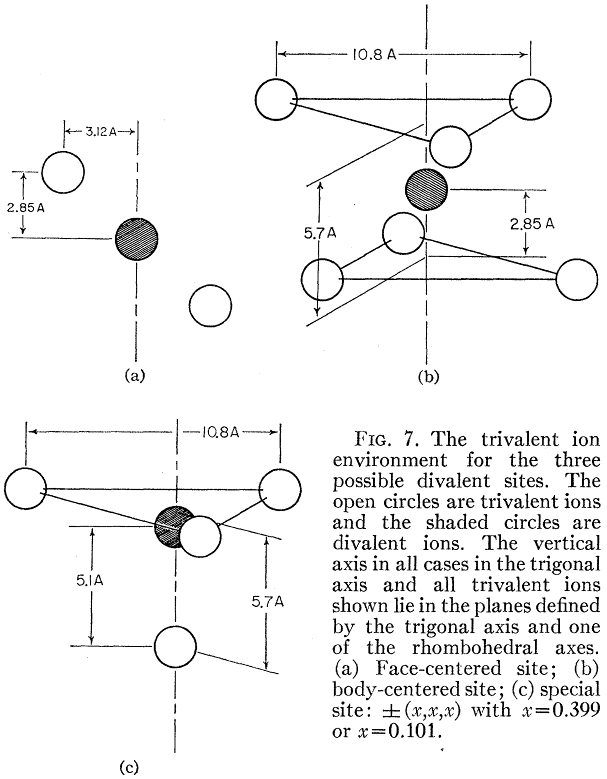

FIG. 7. The trivalent ion environment for the three possible divalent sites. The open circles are trivalent ions and the shaded circles are divalent ions. The vertical axis in all cases in the trigonal axis and all trivalent ions shown lie in the planes defined by the trigonal axis and one of the rhombohedral axes. (a) Face-centered site; (b) body-centered site; (c) special site: $\pm(x,x,x)$ with $x=0.399$ or $x=0.101$.

Face-Centered Site

Despite the fact that occupation of the face-centered sites excludes any other type of site whereas two cobalt spectra are observed, we shall show that there are other grounds for rejecting it as a site for either the X or Y ion.

As shown in Fig. 7(a), the face-centered site has two nearest neighbors. The three ions shown there are in a plane defined by the trigonal axis and one of the three rhombohedral axes. There are six such sites, two in any one plane related by inversion through the center of the cell. Thus the observed line shape will show sixfold symmetry about the trigonal axis, although the individual sites have lower symmetry. When the magnetic field is applied perpendicular to the plane represented in Fig. 7(a), the two cerium spins shown there will produce a ΔH of ± 235 gauss for the two sites in that plane when both spins are parallel or antiparallel to the field. The splittings at the other four sites and those due to next nearest neighbors are much smaller. Thus at $\theta=90°$ and $\phi=30°$, one would expect to observe a strong central component and components one tenth of the amplitude of the central component shifted by ± 235 gauss. Such an effect is in disagreement with the observations for both the X and Y ions.

Body-Centered Site

The trivalent ion environment of the body-centered site is shown in Fig. 7(b). The vertices of the triangles at which the trivalent ions are located are in the planes defined by the trigonal axis and the rhombohedral axes. The maximum splitting ΔH from a single pair of ions is realized when the field direction bisects the vertices of one of the triangles. This direction corresponds to $\theta=90°$, $\phi=0$. However, each of these two spins can contribute only 40 gauss to ΔH, so that the maximum value of ΔH due to these two neighbors is 80 gauss. Further, the other four ions each contribute ± 16 gauss so that the "two neighbor effect" would be suppressed. This site cannot be that of the X ion but it is compatible with the observations for the Y ion.

The Special Site

The special site can produce the line shape observed for the X ion, if the parameter x is given a suitable value. If the distance of the site from the center of the cell is assumed to be either 13.64 A or 3.44 A, the trivalent environment is that shown in Fig. 7(c). The small value of x seems less plausible when considered in terms of the over-all crystal structure because it would lead to a much closer packing of the divalent ions than would the larger value of x. There are two sites related to each other by inversion with respect to the centroid of the triangle.

When the field direction bisects the interior angle at one of the vertices of the triangle ($\theta=90, \phi=0$), the cerium ion at that vertex can contribute ± 69.5 gauss to ΔH. The cerium ion on the trigonal axis and 5.1 A away contributes ± 65 gauss to ΔH whereas the other two nearest neighbors contribute only ± 9.2 gauss. The values of the splitting due to the most effective neighbors will be ± 134.5 gauss and ± 4.5 gauss which is consistent with the observations. At $\theta=90°$ and $\phi=30°$, the fields which the four ions can produce are ± 65, ± 35, ± 35 and ± 28. This will produce very little structure in the derivative of absorption, which is consistent with the observations recorded in Fig. 1(b). The distance of 5.1 A shown in Fig. 7(c) is determined to within about 0.05 A.

This interpretation of the X-ion line shape implies that the outer components of the line correspond to states where the two cerium ions are antiparallel. Thus the relative intensity of the high- and low-field components will be independent of temperature, whereas if these two components required that both spins be either parallel or antiparallel to the field, a temperature dependence would be expected. If the latter were the case, the relative amplitudes of the two components would be 1:0.7 at a temperature of 1.1°K and in a field of 2500 gauss. Under these conditions, no change in the line shape was observed experimentally.

Further Comparison of Experiment and Theory

The mean square magnetic field width due to the secular part of the dipolar interaction between dissimilar anisotropic ions of spin $\frac{1}{2}$ has been calculated for an arbitrary field direction. The calculation is exactly that of Van Vleck[16] except that the two types of spins must be quantized along their axes of precession, which are in general not the same for anisotropic ions. The mean square width, in gauss squared, for the isotropic cobalt resonances due to the interaction with Ce ions is

$$\sigma_d^2=2.37\times10^{-40}(g_{\parallel}^2\cos^2\theta+g_{\perp}^2\sin^2\theta)\sum_j B_j^2,$$

where

$$B_j=\frac{1}{r_j^3}\left(1-\frac{3F_j}{r_j^2(g_{\parallel}^2\cos^2\theta+g_{\perp}^2\sin^2\theta)}\right),$$

and

$$F_j=g_{\parallel}^2z_j^2\cos^2\theta+g_{\perp}^2\sin^2\theta(x_j\sin\phi+y_j\cos\phi)^2 +(g_{\parallel}^2+g_{\perp}^2)\cos\theta\sin\theta(z_jx_j\sin\phi+z_jy_j\cos\phi).$$

The g factors are those of the cerium ions and r_j is the distance in cm to the jth cerium neighbor. The z axis is the trigonal axis of the crystal and the x and y axes are two orthogonal axes in the plane perpendicular to the trigonal axis. The angle ϕ is that between the component of the applied field which is perpendicular to the trigonal axis and the direction of the y axis.

The required dipole sums have been calculated for the body-centered and special sites by summing over all neighbors within a distance of 31 A. For the special site the result can be expressed very simply if we assume $g_{\parallel}=0$. The result is

$$\sigma_d^2=1.07\times10^4\sin^2\theta(1+0.096\,\text{ctn}^2\theta -0.100\,\text{ctn}\theta\cos^3\phi+0.300\,\text{ctn}\theta\sin^2\phi\cos\phi).$$

The square root of this result is compared with experimental results for the X ion as a function of ϕ in Fig. 5 and as a function of θ in Fig. 4. The theoretical variation with the angle θ is insensitive to the value of $g_{\parallel}$ for $\theta>30°$.

The theoretical expression for the splitting ΔH produced for ions in the special site is

$$\Delta H=33.5\{\cos(\theta-\psi)-6\cos\theta\cos\psi +3[\cos(84°-\theta)][\cos(84°-\psi)]\},$$

where $\tan\psi=(g_{\perp}/g_{\parallel})\tan\theta$. The above result is more sensitive to the value of $g_{\parallel}$ than is σ_d and the experimental values are easily within ±5 gauss of the correct values. In Fig. 4, all the experimental points lie between the theoretical curves for $g_{\parallel}=0$ and $g_{\parallel}=0.25$. Accepting the theory, the best value of $g_{\parallel}$ is 0.125. This value is certainly better than we were able to obtain by direct measurement of the cerium resonance, partly because of our limited magnetic field ($<$11 000 gauss). Agreement with the curve for $g_{\parallel}=0$ would require a systematic orientation error of about 5 degrees which is very unlikely.

The rms magnetic field width calculated from the dipole sums for the body-center site is 72 gauss for $\theta=90°$. This is within the experimental limits of 64 and 98 gauss obtained for the Y ion.

IV. CONCLUSIONS

We conclude that if the interaction between the Ce and Co ions is properly described by that between magnetic dipoles, then the X-ion sites are either $\pm(0.399,0.399,0.399)$ or $\pm(0.101,0.101,0.101)$. The extent of agreement between theory and experiment appears to justify the assumption concerning the interaction.

The less extensive data for the Y ion agrees with the predictions for the body-centered site, but may not rule out the possibility of some interstitial site. If the special sites are occupied by cobalt ions, then the body-centered site must be occupied by some divalent ion and it seems unlikely that the cobalt ions would not occupy this site at all. The ratio for the number of X ions to the number of Y ions has been observed to be between 1.5:1 and 2:1. The ratio of special to body-centered sites is 2:1. There seems to be no reason that the ratio of available sites must be precisely the same as the ratio of ions when those ions are present in low concentration.

The only ambiguity remaining in the divalent positions is the two possible values of the parameter x. The smaller value of x corresponds to a structure in which the divalent ions are much more crowded than would be the case for the larger value of x.

The information on the Ce$-$Co interaction given in this paper lays the foundation for a quantitative understanding of the perturbation of the nuclear orientation of Co^{60} by spin-spin interaction with cerium ions.[3–5]

V. ACKNOWLEDGMENTS

We wish to thank Professor Paul W. Gilles of the Chemistry Department for the use of the x-ray facilities supported in part by the U. S. Atomic Energy Commission, as well as advice and suggestions concerning the x-ray measurement. Advice and assistance from Dr. John A. L. Wahl and Mr. Ernest R. Plante in this phase of the work is also gratefully acknowledged.

APPENDIX I. OVERLAPPING HYPERFINE LINES

Dipolar interactions between an ion, the resonance of which is being observed, and neighboring dipoles will lead to a nearly Gaussian line shape if there are a relatively large number of nearest neighbors isotropically distributed.[16] Even in cases where this condition is not met, as encountered in this investigation, essentially Gaussian broadening may be produced by more remote neighbors. In the following, the shape of the derivative of paramagnetic absorption for a series of eight equally spaced hyperfine lines is discussed, and

---

[16] J. H. Van Vleck, Phys. Rev. 74, 1168 (1948).

the methods are described for extracting information from the shape in a simple way. These methods were used to obtain the hyperfine interactions data for the Ce—Zn salt.

The curves generated by the derivative of eight equally spaced Gaussian curves were calculated for a number of values of the ratio of the rms width of the individual Gaussian curves to their spacing. Three of these curves are reproduced in Fig. 3. From these curves one may conclude the following: In those cases where small inner peaks are present, the distance between the two central peaks is precisely the spacing of the individual lines. Further, the ratio of the inner peak heights to those for the outer peaks is a sensitive measure of the ratio of separation to individual linewidth. As the width of the individual components increases their width and their spacing may be inferred from the widths of the outer peaks and the separation of the outer peaks, if the number of components is known. Sensitivity to the spacing is gradually lost as the flat region between the two peaks disappears with increasing component width.

APPENDIX II. UNIT CELL AND SPACE GROUP

X-ray powder diffraction data for Ce—Zn were indexed for a hexagonal unit cell with $c=34.18$ A and $a=10.84$ A. The strong lines of the powder pattern correspond to the hexagonal parameters $c=17.09$ A and $a=10.84$, which are in satisfactory agreement with the parameters reported for Ce—Mg by Powell[17] ($c=17.22$, $a=10.92$).

The extinctions characteristic of a rhombohedral unit cell are observed. The parameters of the rhombohedral unit cell are 13.1 A for the sides and 49° for the interaxial angle. The size of the unit cell and the observed density of the salt implies that there is one molecule per unit cell. The smaller unit cell defined by the strong lines implies that the Ce ions are in the general positions $\pm(\frac{1}{4},\frac{1}{4},\frac{1}{4})$. The unit cell which was deduced from these measurements has been verified for Ce—Mg by Swanson.[18]

The intensities obtained in the present investigation and those obtained by Swanson have been analyzed by a statistical method described by Lipson.[19] This analysis is capable of distinguishing the presence or absence of a center of symmetry. Both sets of data require that the unit cell have a center of symmetry. In addition, a Laue pattern was obtained for the x-ray beam direction along the trigonal axis. This pattern showed that the Laue group is $\bar{3}m$ which includes the rhombohedral space groups $R\bar{3}m$, $R\bar{3}c$, $R32$, $R3m$ and $R3c$. Only the first two of these has an inversion center and $R\bar{3}c$ would have systematic extinctions which would have been detected in the powder pattern. From this it may be concluded that the space group is $R\bar{3}m$ (No. 166).

---

[17] H. Powell (unpublished), quoted in reference 6.

[18] H. E. Swanson (private communication).

[19] H. Lipson and M. M. Woolfson, Acta. Cryst. **5**, 680 (1952).